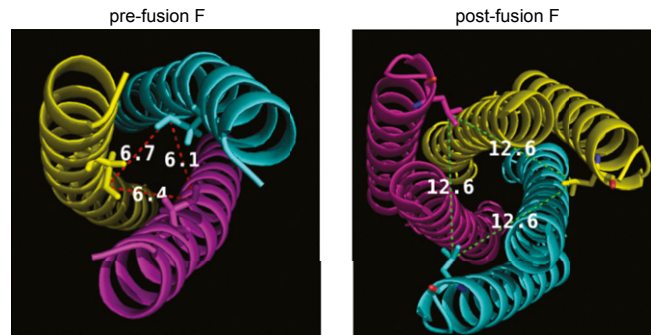
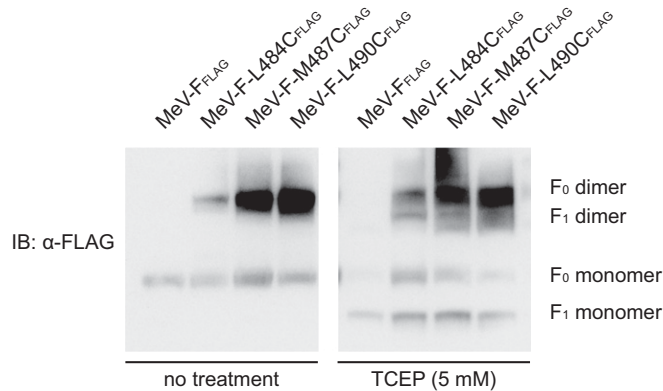


# Supporting Information

Brindley et al. 10.1073/pnas.1403609111



**Fig. S1.** Predicated distances between the sulfur atoms of the engineered cysteines in pre- (*Left*) and postfusion (*Right*) models of paramyxovirus fusion (F) protein. Numbers represent measurement in Angstroms; postfusion distances are measured through the core of the central triple helix of the heptad domain adjacent to the F peptide (HR-A).



**Fig. S2.** Cell monolayers expressing the viral attachment (H) and F proteins were left untreated or were incubated with 5 mM Tris(2-carboxyethyl)phosphine (TCEP) as in the fusion assay in Fig. 2D. Total cell lysates were harvested with RIPA buffer (composition given in *Materials and Methods*) and analyzed through nonreducing SDS/PAGE. The TCEP treatment conditions were designed to be sufficient to reduce a portion of the dimeric surface-expressed F proteins but not to reduce completely all disulfide bonds of proteins present at the cell surface. Higher TCEP concentrations decreased cell-to-cell fusion, presumably because of more complete reduction of endogenous disulfide bonds, and therefore were not applied in this experiment. IB, immunoblot; Mev, Measles virus.

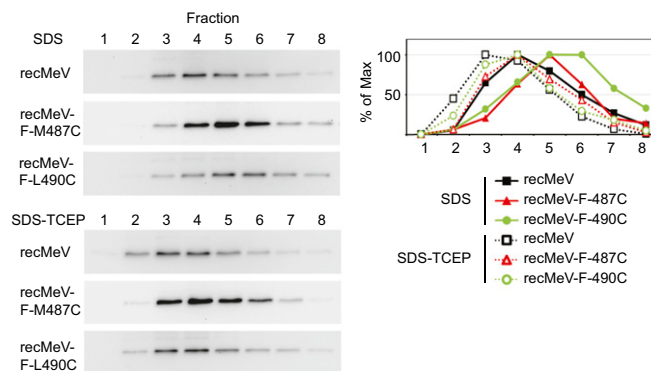


**Fig. S3.** Covalently linked  $F_{\text{cysteine}}$  constructs are incorporated into recombinant MeV (recMeV) virions. (*Left*) Proteins were extracted from purified particles (SDS) or were extracted and reduced (SDS-TCEP), fractionated on a 1–12% iodixanol (1% per step) gradient, and subjected to immunoblotting using  $\alpha$ -Ftail antiserum. Twelve equal fractions were generated and analyzed. (*Right*) Densitometric quantifications of the F-protein material in each fraction are shown, normalized for the fraction with the highest F-protein content.

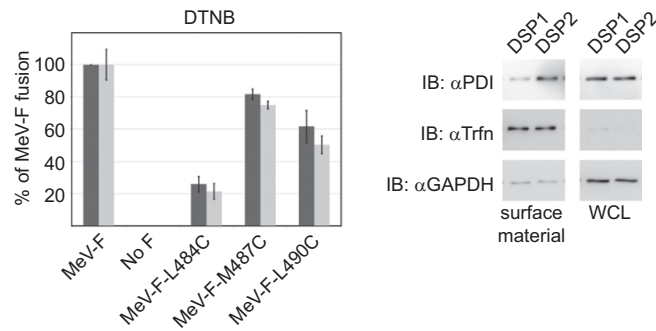


**Fig. S4.** Inhibition of cellular protein disulfide isomerases (PDIs) does not alter  $F_{\text{cysteine}}$ -mediated fusion activity. (Left) Quantitative cell-to-cell fusion assays in the presence (light grey bars) or absence (dark grey bars) of the broad-spectrum PDI inhibitor 5,5'-dithiobis-(2-nitrobenzoic acid) (DTNB). Values shown are averages of at least four experiments  $\pm$  SEM. (Right) PDI-neutralizing monoclonal antibodies (RL90) recognize PDIs displayed on the surface of stably transfected cells expressing dual-split protein 1 (DSP1) and dual-split protein 2 (DSP2). Immunoblots of material obtained through surface biotinylation and whole-cell lysates (WCL) were probed with RL90 monoclonal antibodies ( $\alpha$ PDI) or antibodies directed against the cellular transferrin receptor ( $\alpha$ Trfn) or GAPDH ( $\alpha$ GAPDH).

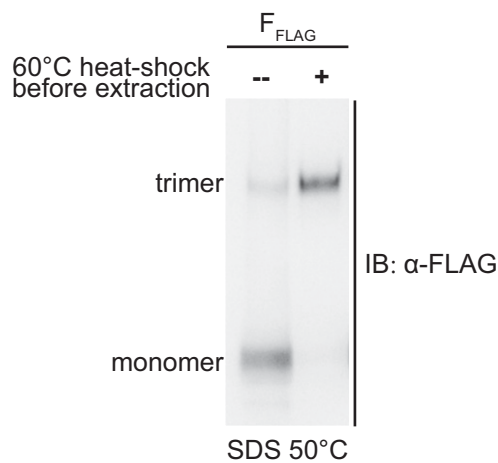


**Fig. S5.** Only postfusion F trimers are resistant to mildly denaturing conditions after native extraction. Cells expressing standard F proteins were cooled directly (–) or were subjected to a 60 °C heat shock followed by cooling (+). Then plasma membrane proteins were natively extracted, subjected to mild denaturing conditions (0.5% SDS 50 °C), and fractionated through nonreducing Tris-acetate-SDS/PAGE. Immunoblots were developed using specific antibodies directed against the FLAG epitope tags ( $\alpha$ -FLAG). The migration pattern of F oligomer forms is indicated.

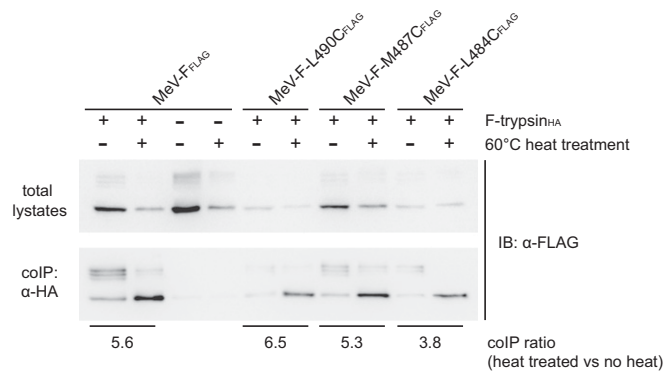


**Fig. S6.** Standard F protein and  $F_{\text{cysteines}}$  form heterotrimers with  $F_{\text{trypsin}}$ . Differentially epitope-tagged standard F or  $F_{\text{cysteines}}$  were coimmunoprecipitated with  $F_{\text{trypsin}}$  after cells were transfected with a mixture of equal amounts of plasmid DNA encoding the different F constructs. Cells were harvested immediately (37 °C) or were subjected to heat shock (60 °C) to induce F-protein refolding before lysis. Lysates were subjected to immunoprecipitation using specific antibodies (16b12) directed against the HA epitope ( $\alpha$ -HA) and were coprecipitated (co-IP) with standard F protein or  $F_{\text{cysteines}}$  identified in immunoblots using  $\alpha$ -FLAG antibodies. Coimmunoprecipitation was more robust after the induction of F-protein refolding, as is consistent with the notion that the postfusion conformation stabilizes F trimers.



**Table S3. Calculations of HR1 (HR-A) and HR2 (HR-B) residue length and HR1/HR2 interface length for a variety of class I viral fusion proteins originating from different viral families**

Protein Data Bank ID code	Virus	Viral family	Residues in HR1 (HR-A)	Residues in HR2 (HR-B)	Ratio HR1/HR2	Length of HR2 (HR-B) helix, Å
1MOF	MoMLV	$\gamma$ -Retroviridae	33	0	ND	0
2XZ3	BLV	$\delta$ -Retroviridae	52	8	6.5	12
1MG1	HTLV-1	$\delta$ -Retroviridae	46	8	5.75	12
4JPR	ASLV	$\alpha$ -Retroviridae	39	16	2.44	24
4JF3	MPMV	Retroviridae	47	22	2.14	33
1JEK	Visna	lenti-Retroviridae	39	33	1.18	49.5
2G2K	MARV	Filoviridae	41	15	2.73	22.5
2EBO	EBOV	Filoviridae	36	14	2.57	21
3MKO	LCMV	Arenaviridae	48	14	3.43	21
4C53	Guanarito	Arenaviridae	44	16	2.75	24
2IEQ or 1ZV8	SARS	Coronaviridae	49	32 or 20	1.53 or 2.45	48 or 30
4MOD	MERS	Coronaviridae	42	17	2.47	25.5
3KPE or 3RRT	RSV	Paramyxoviridae	49	32	1.53	48
3MAW	NDV	Paramyxoviridae	65	26	2.5	39
1SVF	SV5	Paramyxoviridae	60	26	2.31	39
1ZTM	hPIV3	Paramyxoviridae	66	27	2.44	40.5
1WP7	NiV	Paramyxoviridae	34	28	1.21	42
1WP8	HeV	Paramyxoviridae	32	26	1.23	39
2FYZ	MuV	Paramyxoviridae	52	26	2	39

Protein Data Bank ID codes for the individual fusion cores are specified. ND, not determined because of the disorder of the HR2 domain in the crystal structure.